Surg Today (2006) 36:701–706
DOI 10.1007/s00595-006-3232-7

SURGERY TODAY

Evaluation of the Relationship Between the Viscoelastic Stress and Strain of Fetal Rat Skin as a Guide for Designing the Structure and Dynamic Performance of a Manipulator for Fetal Surgery

KOTA TSUBOUCHI[1], SHIN ENOSAWA[2], KANAKO HARADA[1], JUN OKAMOTO[1], MASAKATSU G. FUJIE[1], and TOSHIO CHIBA[3]

[1]Department of Mechanics Engineering, Waseda University, Tokyo, Japan
[2]Department of Innovative Surgery, National Research Institute for Child Health and Development, 2-10-1 Okura, Setagaya-ku, Tokyo 157-8535, Japan
[3]National Center for Child Health and Development, Tokyo, Japan

Abstract

Purpose. To design an endoscopic manipulator for fetal surgery. The viscoelastic properties of fetal skin were estimated from both the viewpoint of mechanical structure and data collection for controlling the device.

Methods. The skin of fetal Wistar rat (19.5 days old) was set on a rheometer and the relationship between stress and strain was examined. Morphological damage was assessed histologically.

Results. The stress–strain curve was nonlinear and sigmoidal throughout the process. The skin fracture point was estimated to be over 4 kPa. After multiple challenges of low-level loading under 150 Pa, the curve showed no detectable change due to mechanical fatigue. Histologically, the basement membrane was not damaged even at the fracture point; however, severe damage to the dermis was observed.

Conclusion. The viscoelastic properties of the fetal rat skin were mainly caused by the dermis and the value of the shear stress that causes skin fracture was estimated to be 4 kPa. To design a robotic stabilizer, limit of mechanical loading was thus tentatively set at 400 Pa, with a 1/10 fracture point.

Key words Rat · Fetal surgery · Skin · Robot · Endoscopic surgery

Introduction

Recent technological progress in prenatal diagnoses[1–4] such as obstetrical ultrasonic diagnosis has led to further innovations in the medical technology related to fetal surgery.[5–9] Myelomeningocele is one promising target condition that lends itself to fetal surgery because the disease is usually a simple malformation without any other serious complications including genetic mutations, and surgical treatment during the fetal stage can result in a marked improvement in the quality of life (QOL) after birth. Conventional surgery for fetuses under a laparotomy has several undesirable aspects, such as an increased risk of massive hemorrhaging, difficulty in controlling the fetal body temperature, the need for special anesthetic care, and fetal anemia or congestion due to the occlusion of the umbilical vessels.

As a result, a new surgical procedure, namely endoscopic robot surgery, has attracted attention because this technique can allow us to overcome some of the disadvantages of conventional surgery. For example, the da Vinci surgical system is able to replace certain types of surgical procedures. Generally, the robot manipulator consists of three parts, i.e., the operator site (master), the interface, and the operating site (slave) (Fig. 1). The roles of interface are (1) to transmit the operator's movement to the point of action, (2) to convey the position of the instrument by a sensory feedback mechanism, and (3) to intercept an excessive load. Therefore, the physiological data input to the interface is indispensable when constructing a robotic surgical device. As a final goal, data accumulation will allow us to optimize the slave movement regardless of the operator's handling.

So far, there have been no trials to develop endoscopic surgical apparatuses specifically for fetal surgery. Besides the size and fragility of the fetus, other difficulties for designing the apparatus are as follows: (1) the fetus is floating in uterine amniotic fluid and thus is hard to keep in place, (2) unlike ordinary endoscopy, the operating field is in liquid, (3) surgical devices such as the electric scalpel and ultrasonic scalpel cannot be used, (4) the insertion point of the manipulator is limited by the position of the placenta, and (5) the visual field of the endoscope is unclear in the stagnant intrau-

Reprint requests to: S. Enosawa
Received: June 10, 2005 / Accepted: March 14, 2006

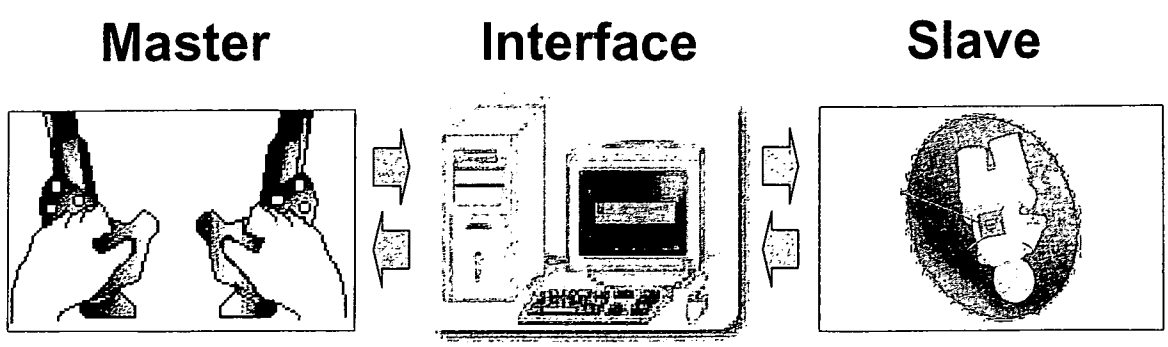

Fig. 1. Overview of the robotic surgery system. This system consists of a master controller, interface, and a slave manipulator. Input from the master controller is fed to the slave manipulator through the interface

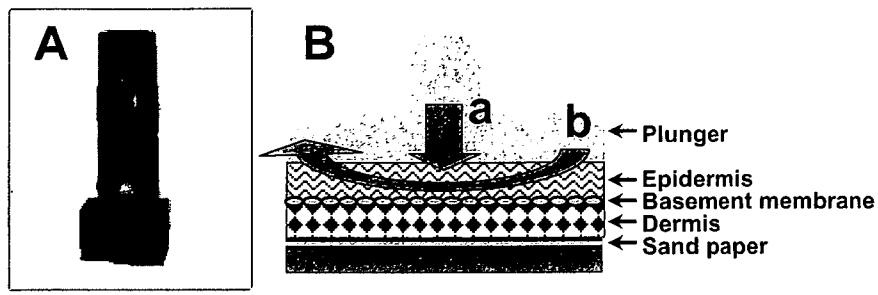

Fig. 2A,B. Outline of the creep test. **A** Rheometer. **B** Schematic illustration of the creep test. The pressure of the geometry plunger was 0.1 N (*arrow a*) and shear stress was loaded from 50 to 4 kPa by rotating the plunger (*arrow b*) for 5 min. The time course change in the plunger movement was recorded as strain

terine amniotic fluid. Among these points, devising a proper holding technique is considered to be the most important factor, not only for designing the operating slave site but also for constructing an appropriate interface program.

The aim of this study was to construct a holding system for the fetal operating field and also to evaluate the mechanical fragility of fetal tissue, i.e., the stress–strain response of the skin. Based on the present data, we herein propose a safety range of surgical stress to fix the operating position and dynamical model of fetal skin tissue.

Materials and Methods

Animals and Fetal Skin Sampling

Both male and female Wistar rats (specific pathogen-free grade) were purchased from Japan Clea (Tokyo, Japan) and mated in our animal facility. Impregnation was confirmed by a smear test. In all experiments, 19.5-day fetuses were used because the rat fetal age of 19.5 days is equivalent to a human fetal age of 20–25 weeks, the time at which fetal surgery is normally performed, according to Witschi's stage classification.[10] After fetuses were taken out by cesarian section under ether anesthesia and decapitated, full-thickness dorsal skin samples (8 × 8 mm) were cut and stored at 0°C in ice until analysis. The range of the storage times was approximately 2–6 h. In one experiment, the skins from approximately 10 rat littermate fetuses were harvested to use for each condition and the data from four independent experiments were compiled. All experimental procedures were performed according to our institutional animal ethics guidelines, which are based on those of the National Institutes of Health of the USA.

Rheometer Analysis

A stress–strain experiment under constant stress, which is called the "creep test" in technological terminology, was performed by using a rheometer (AR-550; TA-Instruments, New Castle, DE, USA) (Fig. 2A). Fetal rat skin was placed on a piece of sandpaper on the specimen tray to fix the skin in position (Fig. 2B). The skin was pressed by a geometry plunger (8 mm in diameter) to 0.1 N (Newton), and shear stress was loaded gradually for 5 min for 50 Pa to 4 kPa by rotating the plunger and evaluating the strain as a ratio of rotation displacement / full circumference. After loading, the shear stress was released and the residual strain was recorded after 5 min following the release of the load. The maximal strain and the residual strain were determined as shown in Fig. 4A.

Histological Examination

Skin samples were fixed with neutralized formalin and microscopic sections were stained with hematoxylin–eosin.

Results

Growth of Rat Fetus

The implantation of rat embryo occurs 5 days after fertilization and the gestational period is around 22.5 days.[10] Figure 3 shows the growth of fetal craniocaudal length and body weight in our animal experiment. The rats were delivered 22.5 days after the day of mating. The craniocaudal length and body weight at the time of delivery were 44.1 ± 1.43 mm and 5.44 ± 0.29 g, respectively. In this experiment, we took skin from day-19.5 fetuses, since this gestational age is equivalent to 20–25 weeks of human gestational age.[10] The craniocaudal length and body weight on day 19.5 were 27.0 ± 1.37 mm and 1.95 ± 0.08 g, respectively, and the ratios to the full-term rats were 61.4% and 35.8%, respectively.

Stress and Strain Curve by Creep Test

A typical time-course curve of the strain change is shown in Fig. 4A. Approximately during the first second, the strain rose rapidly to a particular level (approximately 1/3 of the maximal strain) depending on the elasticity of the sample due to the initial elastic potential of the skin and then, after a brief oscillation period (~6 s) (Fig. 4B), the value increased logarithmically. The maximal strain was defined expediently as the value at 5 min after the start of loading, which corresponded to the point when the equilibrium of strain was approximately attained (Fig. 4A). After the release of stress, the strain decreased logarithmically during the recovery stage and then converged to the residual strain, thereby indicating the degree of irreversible change of skin after stress loading. Based on the time-course curve of strain, the mechanical-dynamical model shown in Fig. 4C was plotted. The skin model is composed of springs (elasticity) and dumpers (viscosity) connected serially and in parallel.

The relationship between stress and maximal strain is shown in Fig. 5A. Three independent experiments were performed up to a fracture point and the maximal and residual strain was plotted. A nonlinear sigmoidal relationship was observed throughout the process and the curves were similar. The skin fracture point was revealed by the skidding of the plunger and was estimated to be approximately 4 kPa, i.e., 4 g per cm², the value of which is approximately equivalent to the power needed to penetrate 10% soft gelatin by a finger (preliminary observation, not shown).

Figure 5B shows a plot of strain as a function of the repeated loading of shear stress. Closed circles denote the maximal strain and open circles residual strain. The standard deviation (SD) of five measurements for each

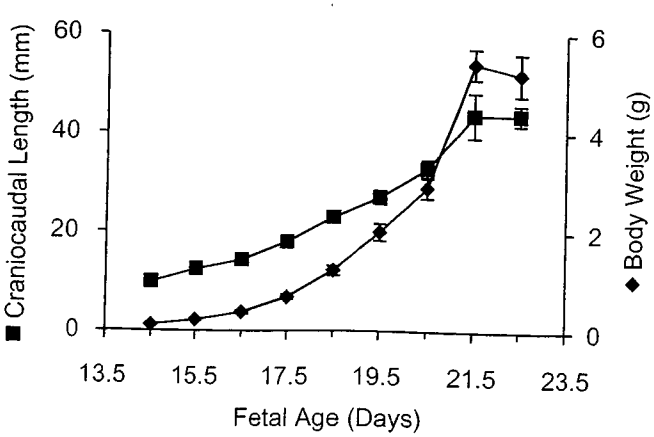

Fig. 3. Growth curve of the rat fetus in body weight (*diamonds*) and craniocaudal length (*squares*). The data were obtained in 15–20 fetuses from 3–4 pregnant rats

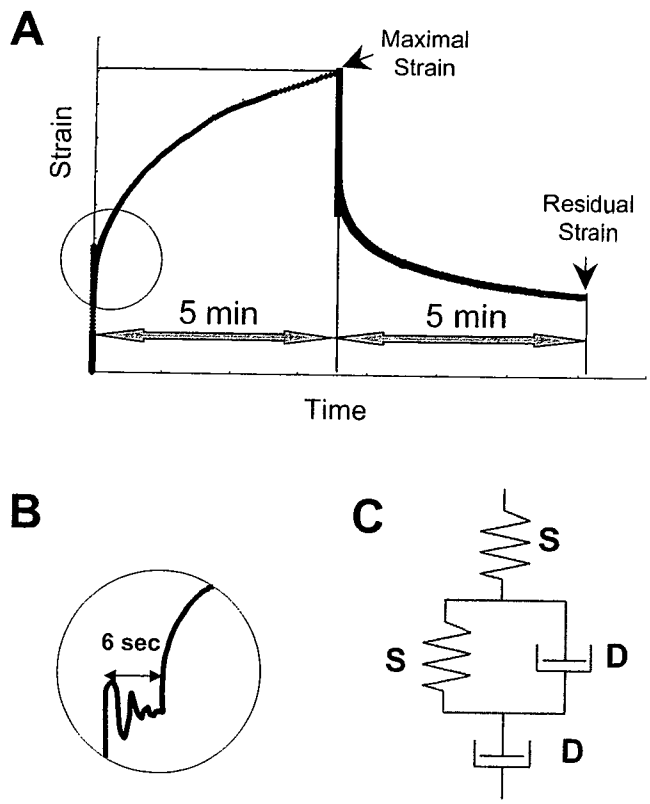

Fig. 4A–C. Stress–strain curve of fetal rat skin. **A** Typical time course change of strain in the creep test. The sample was loaded with a constant load of 100 Pa of shear stress for 5 min, and then was released for 5 min. **B** Magnification of the initial change (area within circle in **A**). The maximal point at the end of 5 min stress loading and residual strain after 5 min release were recorded. **C** The mechanical-dynamical model was drawn based on the stress–strain relationship. The skin model is composed of springs (*S*) (elasticity) and dumpers (*D*) (viscosity).

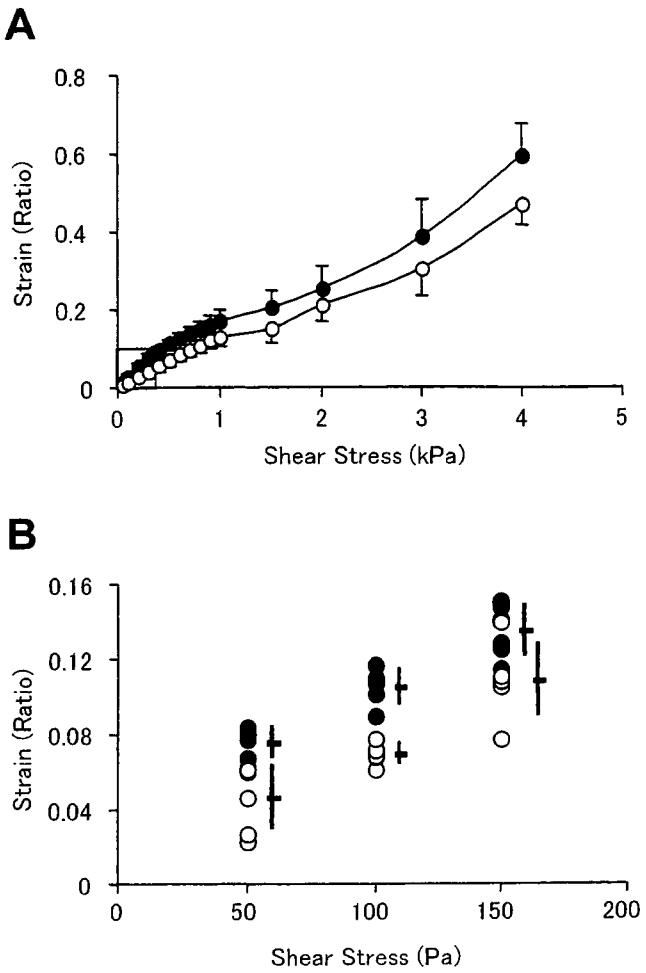

Fig. 5A,B. The relationship between shear stress and strain. **A** The mean maximal strain (*closed circle*) and residual strain (*open circle*) obtained from three independent experiments were plotted. The *bars* indicate SD. **B** The strain values when skin was loaded repeatedly (five times) with the same shear stress. The respective strain values were plotted (maximal strain, *closed circle*; residual strain, *open circle*). The *bars* indicated the mean ± SD

of the two strains was not greater than the individual variations of skins from different fetuses. For instance, the SD of maximal strain in repeated experiments was not greater than the deviation of the individual specimen difference (0.215, 0.255, 0.354 vs 0.348, 0.865, 1.353 at 50, 100, 150 Pa, respectively), i.e., the shear stress of the putative safety range did not induce mechanical fatigue in the skin. The same tendency was observed with residual strain.

Histological Observations of the Fetal Skin After Mechanical Stress

Microscopic studies of fractured skin are shown in Fig. 6. Unlike intact skin (Fig. 6A), there were cracks in the epidermis (arrows in Fig. 6B). However, most of the basal layer remained intact even beneath the damaged area (arrowhead in Fig. 6B). The damage in the dermis was much more severe than in the epidermis (Fig. 6C). Figure 6D shows the skin after five times of repeated loading of 150 Pa. There was no observable histological change, which was consistent with the lack of evidence of mechanical fatigue as shown in Fig. 5B.

Discussion

To develop microsurgical manipulators, it is important to input the data regarding the response of soft tissue against the surgical procedure as well as to design the device hardware. In a classical macroscopic operation, device control depends upon the operator's senses, based on direct feedback from the point of action. As a result, the improvement was mainly concerned with morphological design. However, a microscopic operation such as endoscopic surgery needs a programmed regulation that is independent from human sensing. In other words, artificial feedback from the manipulator is necessary for the smooth and harmonized movement by the operator. The present experiments provided the basic data for the establishment of manipulator regulation.

In humans, the body length and weight at weeks 20–25 as a percentage of those of newborn infants just after delivery are 56.4%–64.0% and 19.7%–21.7%,[11] respectively, thus suggesting that the 19.5-day fetus is a reasonable choice for the period of gestation.

The operation for myelomeningocele needs highly careful techniques to retain, exfoliate, cut, and suture soft fetal tissues,[12,13] and the introduction of robotic surgery will lead to invaluable innovations in this treatment. So far, most investigators have determined the elasticity of soft tissue in order to estimate morphologic change. In the present report, we evaluated not only the dynamics but also the histological changes caused by the viscoelastic properties of fetal skin. Viscosity differs from elasticity in that it includes the factor of time and, therefore, we used a rheometer instead of a simple tension tester.

Moreover, a histological examination revealed that the viscoelastic response was mainly caused by the dermis, and not the epidermis in nature. Interestingly, the basement membrane, the epidermal stem cell layer, remained almost completely intact even after the loading of fracture-level stress, thus suggesting that the regenerative activity is restored. It has been postulated that the dynamic response of soft tissue such as the skin consists of elasticity and viscosity.[15] Since the dermis is composed of collagen fibers and elastic fibers, these two different physical properties result in a complex response against shear stress, as indicated in the strain

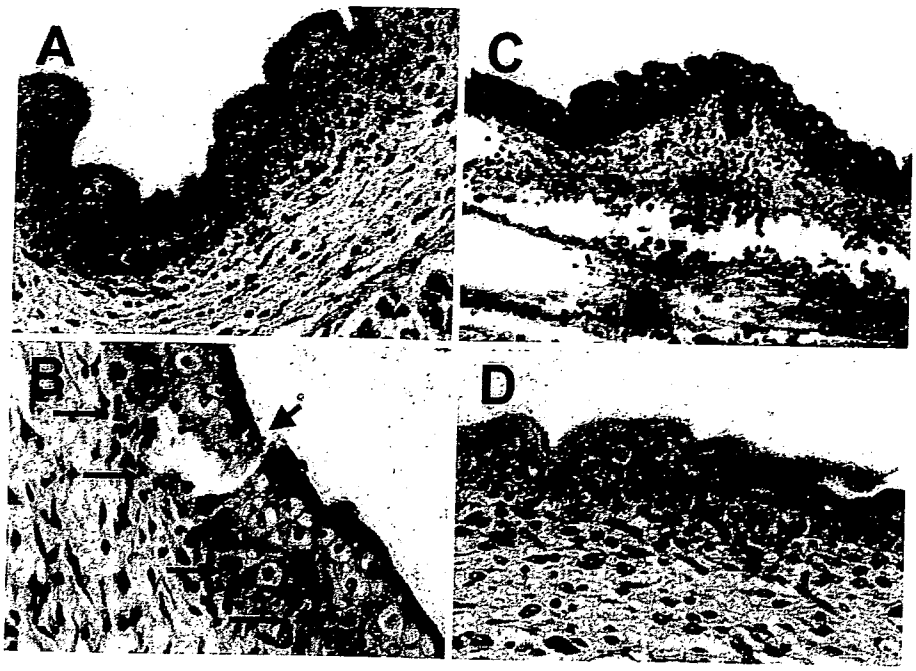

Fig. 6A–D. Histological observation of the fractured fetal rat skin after the creep test. **A** Normal fetal skin. **B** Skin fractured with 4kPa of shear stress loading. Spotty damage was seen in the epidermis (*arrows*). In spite of the intense damage to the epidermis, the basal lamina remained intact (*arrowhead*). **C** Fractured dermis. The damage was much more severe in the epidermis. **D** Skin after five repeated loadings of 150Pa. There was no observable change. Original magnification: **A** ×100; **B** ×40; **C** ×200; **D** ×100

curve. Based on the present data, we herein propose an original mechanical-dynamical model which is composed of springs and buffers (Fig. 4C); however, the biological elements responsible for elasticity and viscosity remain to be elucidated.

A key principle in any surgical procedure is to avoid the crushing and grinding of the tissue. Since the fetus is floating in amniotic fluid in the uterus and is thus hard to hold in position, the retention of the fetus or the operation area should be ensured to achieve effective surgical treatment. Therefore, the present data will be useful for designing a stabilization system. The skin did not show the strain change with multiple stress challenge of low-range stress. Judging from the proposed mechanical-dynamical model (Fig. 4C), the stress–strain relationship is exponential rather than linear, and the safety limit was set up at a 1/10 fracture point at present, but further precise considerations are called for. According to our preliminary experiments, the fracture point was equivalent to the force which caused irreversible change to 10% gelatin. It is therefore likely that the nondamaging retention of the fetus is attainable inside the tentative safety range.

To develop a robotic manipulator as shown in Fig. 1, there remain mechanical difficulties to overcome. For instance, some hinges must turn more than 90° to work in the narrow in-utero space and the material should be compatible with other medical tools, such as those used in such as magnetic resonance imaging. The present data on fetal skin should enable us to design and develop appropriate tools for necessary skin manipulations.

References

1. Harknes UF, Mari G. Diagnosis and management of intrauterine growth restriction. Clin Perinatol 2004;31:743–64.
2. Goncalves LF, Espinoza J, Mazor M, Romero R. Newer imaging modalities in the prenatal diagnosis of skeletal dysplasias. Ultrasound Obstet Gynecol 2004;24:115–20.
3. Moore C, Promes SB. Ultrasound in pregnancy. Emerg Med Clin North Am 2004;22:697–722.
4. Shaikh MS, Lombay B. Fetal MRI: reviewing the history, indications, technique, safety and drawbacks. J Coll Physicians Surg Pak 2004;14:576–9.
5. Chiba T, Albanese CT, Jennings RW, Filly RA, Farrell JA, Harrison MR. In utero repair of rectal atresia after complete resection of a sacrococcygeal teratoma. Fetal Diagn Ther 2000;15: 187–90.
6. Chiba T, Albanese CT, Farmer DL, Dowd CF, Filly RA, Machin GA, et al. Balloon tracheal occlusion for congenital diaphragmatic hernia: experimental studies. J Pediatr Surg 2000;35:1566–70.
7. Abramson LP, Gerber S, Chen YH, Crawford SE. Fetal constrictive pericardial defect with pulmonary capillary hemangiomatosis. J Pediatr Surg 2002;37:1512–4.
8. Fowler SF, Sydorak RM, Albanese CT, Farmer DL, Harrison MR, Lee H. Fetal endoscopic surgery: lessons learned and trends reviewed. J Pediatr Surg 2002;37:1700–2.
9. Harrison MR, Adzick NS, Longaker MT, Goldberg JD, Rosen MA, Filly RA, et al. Successful repair in utero of a fetal diaphragmatic hernia after removal of herniated viscera from the left thorax. N Engl J Med 1990;322:1582–4.
10. Witchi E. 67. Development: rat. In: Altman PL, Dittmer DS, editors. Growth — biological handbook. Fed Am Soc Exp Biol; 1962. p. 304–5.
11. Singer DB, Sung CR, Wigglesworth JS. Fetal growth and maturation: with standards for body and organ development in: Wigglesworth JS, Singer DB, editors. Textbook of fetal and perinatal pathology. 2nd ed. Malden: Balckwell Science; 1998. p. 24–9.

12. Sutton LN, Adzick NS. Fetal surgery for myelomeningocele. Clin Neurosurg 2004;51:155–62.
13. Danzer E, Johnson MP, Wilson RD, Flake AW, Hedrick HL, Sutton LN, et al. Fetal head biometry following in-utero repair of myelomeningocele. Ultrasound Obstet Gynecol 2004;24:606–11.
14. Miller K, Chinzei K, Orssengo G, Bendnarz P. Mechanical properties of brain tissue in-vivo: experiment and computer simulation. J Biomech 2000;33:1369–76.
15. Fung YC. Biomechanics: mechanical properties of living tissues. 2nd ed. Berlin Heidelberg New York: Springer; 1993. p. 242–314.

an Article from

Journal of Robotics and Mechatronics

4F Toranomon Sangyo Bldg., 2-29, Toranomon 1-chome, Minatoku, Tokyo 105-0001, Japan
Tel. +813-3508-0051, Fax: +813-3592-0648, E-mail: robot@fujipress.jp
homepage URL: http://www.fujipress.jp/JRM/

Paper:

Micro Manipulator and Forceps Navigation for Endoscopic Fetal Surgery

Kanako Harada*,, Kentaro Iwase*, Kota Tsubouchi*, Kousuke Kishi*,***, Tetsuya Nakamura****, Toshio Chiba**, and Masakatsu G. Fujie***

*Waseda University
E-mail: hkanako@suou.waseda.jp
**Department of Strategic Medicine, National Center for Child Health and Development
***Mechanical Engineering Research Laboratory, Hitachi, Ltd.
****PENTAX Corporation

[Received November 8, 2005; accepted February 7, 2006]

In this report, we propose newly devised surgical assistance for endoscopic fetal surgery using a micro manipulator and a new forceps navigation system. For this purpose, we fabricated a prototype of a micro manipulator 2.4mm in diameter. The manipulator on which a laser fiber is mounted bends in any direction using ball joints driven by four wires. We also developed a forceps navigation system in which computer graphics can indicate forceps positions even when they stay outside the endoscopic view. This navigation is expected to make endoscopic surgery much more feasible.

Keywords: surgical robot, fetal surgery, safety, navigation

1. Introduction

The recent advances in prenatal diagnosis have made more accurate identification of fetuses with treatable abnormalities [1,2]. Fetal treatment is particularly justified for diseases which probably deteriorate in utero if untreated prenatally. Fetal surgery is expected to less expensively improve the perinatal/life-long prognosis of those affected infants. Historically, interventional procedures for fetal surgery initially focused on open surgical techniques which include invasive maternal laparotomy and hysterotomy. Fetoscopic surgery has been increasingly introduced since 1980 in the hope that less invasive procedure might improve therapeutic outcomes with shorter hospital stay and smaller expenses [3]. However, underwater use of conventional surgical instruments with restricted fetoscopic views and 2-dimentional sonographic navigation imposes varied technical difficulties including floating fetuses, low operability of surgical instruments, limited intrauterine perspective, and extreme vulnerability or fragility of fetal tissues. We propose an innovative surgical assistance for endoscopic achievement of less invasive and more accurate fetal surgery. Our newly integrated in utero surgery system is based on a bending manipulator for laser tissue ablation and a forceps navigator using computer graphics (CG).

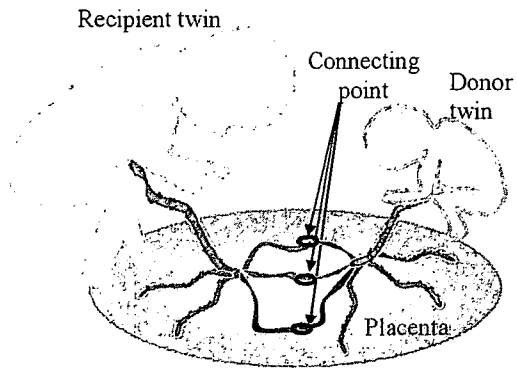

Fig. 1. TTTS.

2. Intrauterine Fetal Surgery

2.1. Goals

Our research goals are to develop safer and faster operative procedures for laser photocoagulation of placental vessels in twin-twin transfusion syndrome (TTTS) [4] and fetal repair of myelomeningocele (MMC) [5,6]. Reportedly, TTTS is seen in 10-15% of monochorionic diamniotic twin pregnancies (single placenta and two amniotic sacs). Almost always, the monochorionic placenta has communicating vessels between both twins and, in TTTS, one twin (donor) and the other (recipient) share abnormal net blood flow with resultant circulatory imbalances as shown in **Fig.1**. The donor is accompanied by significantly less renal blood supply resulting in definitely decreased amniotic fluid (oligohydramnios), whereas the recipient with frequent heart failure as well as much increased renal blood flow presents with a large amniotic fluid volume (polyhydramnios) ultrasonogfraphically. Accordingly, without any prenatal treatment, both twins are likely to die or have irreversible brain damages.

Currently, an increasingly accepted treatment is laser coagulation of placental communicating vessels. Using a single laser fiber mounted on a fetoscope, intrauterine photocoagulation of responsible vessels is carried out on the placental surface. When the placenta is located anteriorly (anterior placenta, 40%), an available window on the maternal abdominal wall is occasionally quite limited to avoid intraoperative placental injury. We propose a micro manipulator that bends laser fiber freely inside the uterus for treating TTTS with anterior placenta (**Fig.2**).

Myelomeningocele (MMC) is congenital anomaly having spinal bone defects with open spinal canal. An inevitable prenatal injury to the exposed spinal code worsens peri-/postnatal infant's neurologic function with resultant life-long disabilities including lower extremity paralysis, dysuria, hydrocephalus (brain disorder). MMC which is usually non life-threatening is one of the most common birth defects. Surgical closure or patch coverage of the spinal defects during mid-gestation have been expected the best way to alleviate postnatal disabilities. Both open and fetoscopic surgeries have been clinically attempted to prevent prenatal spinal cord damages. Here, we propose further less invasive fetoscopic laser surgery to cover the exposed spinal code by agglutinating a collagen patch onto the fetal skin in a quick and water-tight manner (**Fig.3**).

2.2. Technical Problems in Intrauterine Fetal Surgery

The technical problems unique to the intrauterine fetal surgery exist in addition to problems in other forms of minimally invasive surgery as follows [7]:

1) The fetus in the target gestation is very small (the weight of 250-650g) and fragile.
2) A fetus is floating in amniotic fluid in the uterus with unstable position and posture.
3) An available insertion window for surgical instruments' insertion depends on the location of the placenta and the allowable space for instruments' movement within the uterus is limited.
4) The endoscopic view is unclear due to the physiologically cloudy amniotic fluid.
5) The performance of common surgical instruments, such as an electric scalpel, is limited in amniotic fluid.
6) Stimulus to the uterus or fetus could lead to premature delivery.
7) A flaccid uterus under anesthesia is always at risk of massive bleeding.
8) The mother under surgical operation is also at risk of infection and a lost next chance of pregnancy.
9) The use of a thin fetoscope narrows the field of view and makes it difficult to grasp the position of surgical instruments especially when they stay outside the endoscopic view.

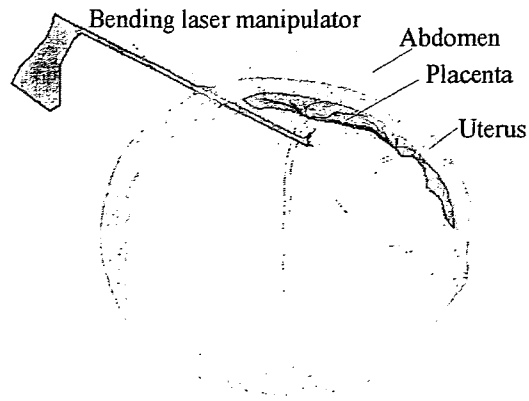

Fig. 2. Manipulator for intrauterine TTTS laser therapy.

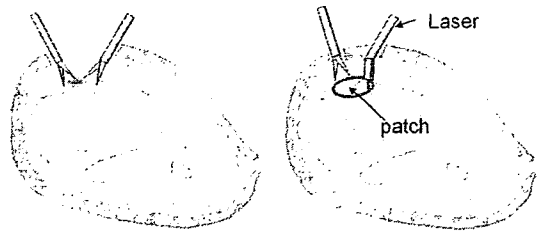

Fig. 3. Open (left) and intrauterine (right) surgery for MMC.

2.3. Surgical Assistance for Intrauterine Fetal Surgery

Many studies conducted to enhance the endoscopic operability have led to some clinical commercialization of surgical robots [8], and these robotic techniques are expected to be introduced in minimally invasive fetal surgery. Reports on experiments applying commercial surgical robots to fetal animal surgery examined the feasibility of robotic fetal surgery but encountered many problems [9, 10]. Commercial surgical robots of 5mm or more are too big for the fetal size and allowable surgical space. One report found that although a surgical robot is costly and requires long setup time, clinical outcomes differ little between robotic and manual surgery. In addition, conventional navigation systems are not available for a mobile fetus and the resolution of intraoperative sonographic images are too low to locate of instrument's distal tip. Our approach is to develop an inexpensive, handheld micro manipulator for dexterous manipulation and a forceps navigation system to help surgeon grasp the surgical instruments' position.

3. Micro Manipulator

3.1. Design

When an incision in the uterus is less than 3mm, it need not sutured, since the contractive force of the uterus itself closes the small hole unaided. A trocar directly inserted into the uterus should have an outer diameter of 3mm or

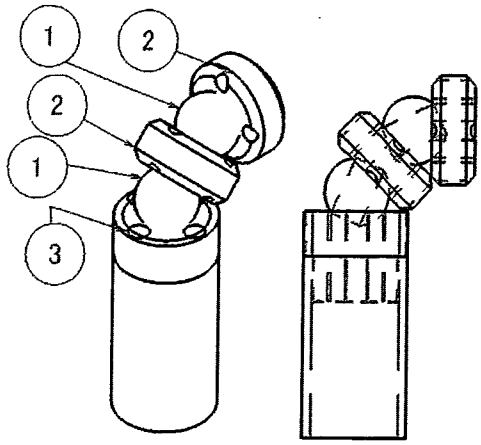

Fig. 4. Manipulator design (1: Ball with through hole, 2: Bending components, 3: Part inserted into a pipe: Each part of 2 and 3 has four holes for the wire path).

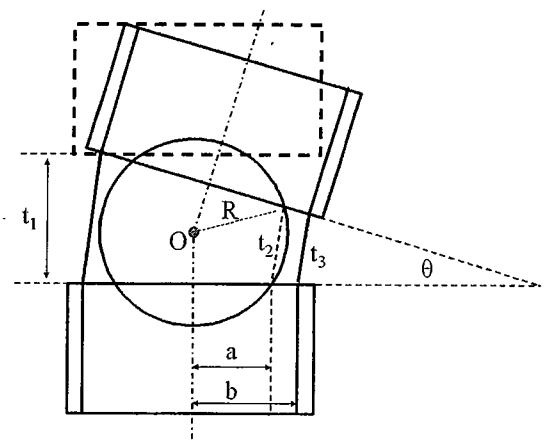

Fig. 5. Wire-pull length versus bending angle.

less, and then we designed a micro manipulator with an outer diameter of 2.4mm. The designed manipulator has two degrees of freedom (DOF) bending at its distal tip for improved operability (**Fig.4**). Ball joints are used to bend in any direction by four wires. The micro manipulator includes an inner hole through all ball joints for the insertion of other surgical applications such as a laser fiber. The micro manipulator has a diameter of 2.4mm and a bending radius of 2.45mm. The features of this mechanism include small diameter and bending radius, ease of fabrication, and high rigidity, and low cost for manufacturing compared to other bending mechanism (wire drive [11, 12], shape memory alloy drive [13], etc.).

Figure 5 shows the bending mechanism as follows:

- t- Wire-pull length of each joint
- t_1- Maximum distance between joints
- t_2- Distance between contact wires of ball and joint
- t_3- Wire length between joints
- R- Distance between ball centers and wire guide
- θ- Bending angle of bending parts
- O- Center of ball

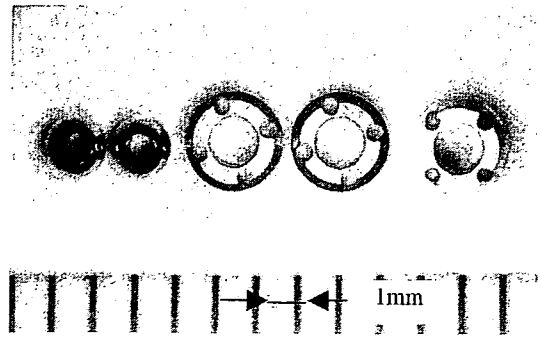

Fig. 6. Bending mechanism components.

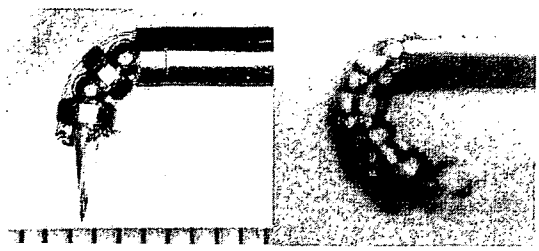

Fig. 7. Micromanipulator prototype.

- a- Distance from contact wire between ball and joint to joint center
- b- Distance between joint center and wire guide center

$$t_1 = 2(R^2 - a^2)^{1/2} \quad (1)$$

$$t_2 = t_1 \cos(\theta/2) - 2a\sin(\theta/2) \quad (2)$$

$$t_3 = t_2 - 2(b-a)\sin(\theta/2) \quad (3)$$

$$\begin{aligned} t &= t_1 - t_3 \\ &= t_1 - t_1\cos(\theta/2) + 2a\sin(\theta/2) \\ &\quad +2(b-a)\sin(\theta/2) \\ &= 2(R^2 - a^2)^{1/2}(1 - \cos(\theta/2)) + 2b\sin(\theta/2). \end{aligned} \quad (4)$$

When the joint number is N, pull length T and entire bending angle Θ are expressed as follows:

$$\begin{aligned} T = 2N\{&(R^2 - a^2)^{1/2}(1 - \cos(\Theta/2N)) \\ &+b\sin(\Theta/2N)\}. \end{aligned} \quad (5)$$

3.2. Fabrication

Components of the fabricated bending mechanism are shown in **Fig.6**, the assembled bending mechanism in **Fig.7**, and the bending mechanism on which a laser fiber is mounted in **Fig.8**. The laser fiber is 0.4mm in laser core diameter and 0.7mm in outer diameter. The maximum bending angle was limited to 60° due to the allowable fiber bending radius. We designed its user interface as handheld type so that the bending angle is controlled at one touch (**Fig.9**). Focusing on enhancing DOF at manipulator's tip reduces its cost and setup time compared to big, master-slave type surgical robots. We used two ultrasonic motors generating high torque at low speed to drive bending, and controlled them with a PC104 (**Fig.10**).

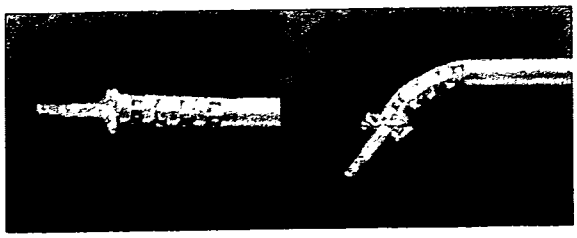

Fig. 8. Bending laser manipulator tip.

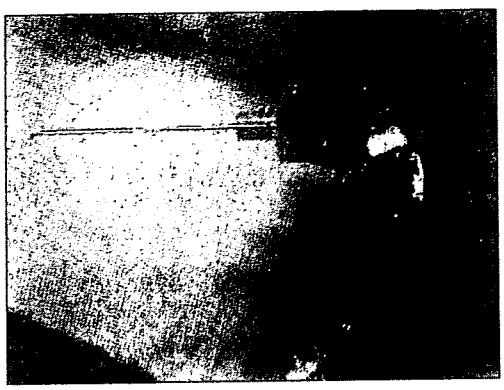

Fig. 9. Bending laser manipulator.

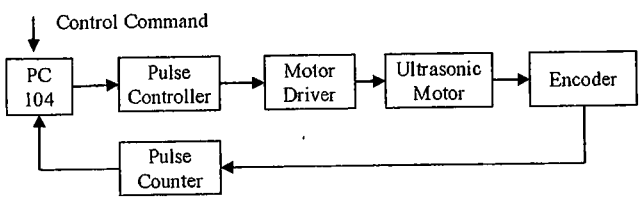

Fig. 10. Motor control.

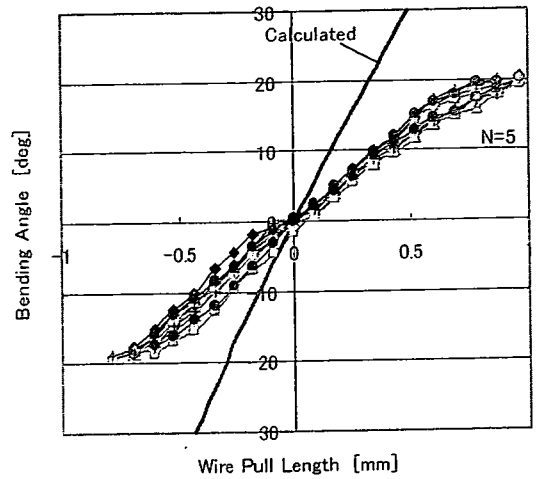

Fig. 11. Bending angle evaluation.

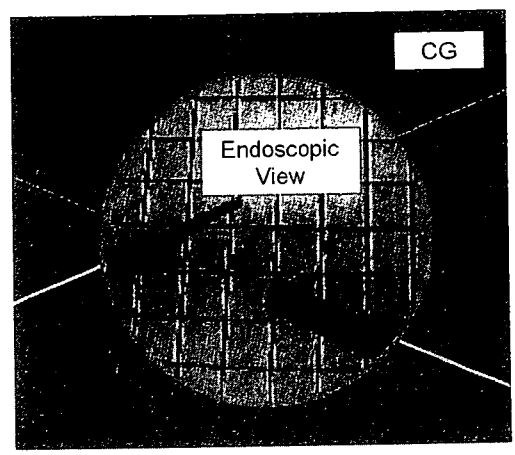

Fig. 12. Forceps navigation.

3.3. Evaluation

Figure 11 shows the result of bending laser manipulator's evaluation. The tip of the manipulator was moved starting at 0° and up to +20° then moved to −20° ending at 0°. This motion was repeated five times and measured with a microscope. The observed hysteresis was due to laser fiber rigidity and the gap between the laser fiber and bending mechanism. The unit drive angle was within three degrees and is sufficiently accurate in relative positioning.

4. Forceps Navigation

4.1. System Configuration

The thin endoscope or fetoscope is used to minimize the incision for tool insertion, but the field of view is reduced and even the slightest forceps movement could make its distal tip go out of the endoscopic field, potentially damaging peripheral tissues outside the field of view. Moving the forceps from outside the endoscopic field inside makes it difficult to predict its position, angle, and speed, lowering surgical instrument operability. We therefore propose forceps navigation system using CG displayed with an endoscopic image (**Fig.12**). An endoscopic image is usually presented as a circularly cutting off image to mask the distorted image area. In the proposed forceps navigation, CG created with OpenGL® (Silicon Graphics, Inc.) are shown in the masked area to indicate the location of forceps tips. Most conventional microscopic or endoscopic navigation present endoscopic images overlayed with CG and this affects the intraoperative observation. Moreover, such navigation requires pre-registration between a patient and preoperative images. Here, we propose a minimum system configuration to grasp the relative position between an endoscope and surgical instruments without intraoperative registration procedures. This navigation is applied to surgery with both conventional instruments and hand-held surgical robots.

4.2. Position Detection

We used the optical position measuring device OPTOTRAK® (Northern Digital Inc.) to detect forceps

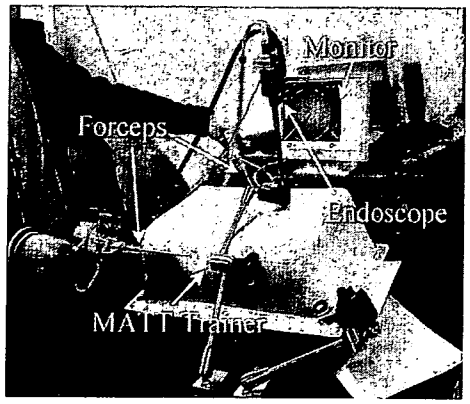

Fig. 13. Experimental view.

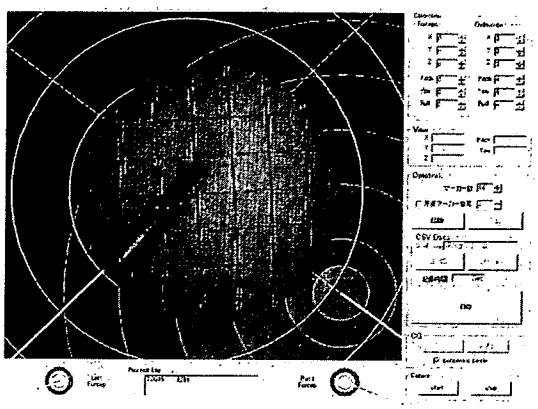

Fig. 14. Forceps navigation with CG.

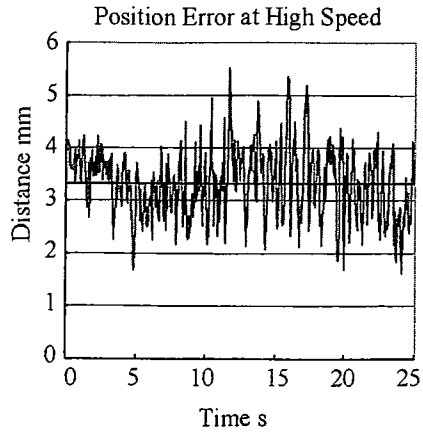

Fig. 15. Accuracy of forceps tip measurement (high-speed).

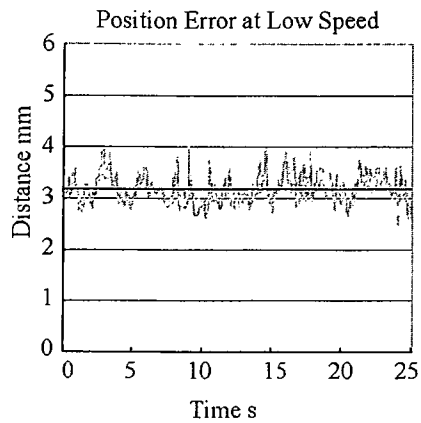

Fig. 16. Accuracy of forceps tip measurement (low-speed).

3-dimensional positions (**Figs.13** and **14**). In **Fig.13**, the base of the forceps with infrared OPTOTRAK® makers are observed enabling the forceps tip in the body cavity to be calculated. The center of the concentric circle given by the CG indicates the tip of the forceps with the diameter of the circle varying according to the distance between the endoscope's tip and forceps' tip in depth direction. The straight line passing through the center of the circle indicates the forward direction of the forceps. We used an indication format similar to a map contour for intuitive presentation. Simple 2-dimensional CG was chosen instead of 3-dimentional CG so that surgeons are less conscious of position detection error or noise.

4.3. Evaluation

The forceps was moved at random by seven subjects and the difference was evaluated between forceps tip position calculated from the makers on the base of the forceps and that measured using makers on the tip of the forceps (**Figs.15** and **16**).

The average accuracy was 3.33mm in high-speed movement and 3.19mm in low-speed movement, thus the average accuracy is less dependent on the speed of movement. This difference was due to the initial positioning error for maker attachments. Although slight fluctuation was observed during high-speed movement, the accuracy of approximately 3mm is enough to grasp the rough position, angle, and speed of the forceps outside the endoscopic field.

Table 1. Results of subjective evaluation (Subjects: 6, Evaluation score: −3 to +3).

	without CG	with CG
Operabirity of the system	−2.3	1.8
Perception of depth	−2.7	−0.3
Anticipation of forceps position	−2.3	2.0
Surgical speed	−2.2	1.3
Feeling of Stress	−1.7	1.3
Operation difficulty	−2.3	0.2

Qualitative evaluation was conducted to ask six subjects to move forceps with/ without CG for 10 minutes and filled out a questionnaire scoring following six items: operability of the system, perception of depth, anticipation of the forceps position, surgical speed, feeling of fatigue, and operation difficulty. The score for each item was given from −3 to +3 points and the result is listed in **Table 1**. We found that the CG navigation greatly contributed to the high evaluation of operability and anticipation of the forceps position.

5. Conclusion

We have developed a micro manipulator and a forceps navigation system for minimally invasive endoscopic fetal surgery. The bending laser manipulator of 2.4mm in diameter was fabricated and the experiment demonstrated its precise positioning. The evaluation of the forceps navigation showed that CG navigation is useful especially for high operability and anticipation of the forceps position. Forceps navigation has not applied to the bending motion so far, but the position of the bending manipulator's distal tip will be calculated in synchronization with the motor control. Integrated surgical assistance with the combination of the micro manipulator and a forceps navigation system will lead to safer and less invasive fetal surgery.

Acknowledgements

This study was in part supported by the 21st Century COE Program "Symbiosis of People and Robotic Technology in the Super Aged Society" of the Japan Society for the Promotion of Science, program "Research on medical devices for analyzing, supporting and substituting the function of human body" by Ministry of Health, Labour and Welfare, and the Intelligent Cluster Creation Project in the Gifu and Ohgaki Regions.

References:

[1] M. R. Harrison et al., "The Unborn Patient: The Art and Science of Fetal Therapy," Elsevier Science Health Science div, 2001.

[2] M. R. Harrison, "The Unborn Patient: Prenatal Diagnosis and Treatment," Elsevier Science Health Science div, 1991.

[3] E. Danzer, R. M. Sydorak, M. R. Harrison, and C. T. Albanese, "Minimal access fetal surgery," European Journal of Obstetrics & Gynecology and Reproductive Biology, Vol.108, Issue 1, pp. 3-13, May 1, 2003.

[4] L. Y. Wee, and N. M. Fisk, "The twin-twin transfusion syndrome," Seminars in Neonatology, Vol.7, Issue 3, pp. 187-202, June, 2002.

[5] N. Tulipan, "Intrauterine closure of myelomeningocele: an update," Neurosurgery Focus, Vol.16, pp. 1-4, February, 2004.

[6] J. P. Bruner, N. B. Tulipan, W. O. Richards, W. F. Walsh, F. H. Boehm, and E. K. Vrabcak, "In utero Repair of Myelomeningocele: A Comparison of Endoscopy and Hysterotomy," Fetal Diagnosis and Therapy, Vol.15, pp. 83-88, 2000.

[7] T. Chiba, M. R. Harrison, C. T. Albanese, and D. L. Farmer, "Fetal Surgery: Past, Present, and Future," Fetal Surgery Japan Society of Prenatal and Neonatal Medicine, Vol.36, No.4, pp. 524-539, 2000.

[8] K. Cleary, and C. Nguyen, "State of the Art in Surgical Robotics: Clinical Applications and Technology Challenges," Computer Aided Surgery, November, 2001.

[9] O. S. Aaronson, N. B. Tulipan, R. Cywes, H. W. Sundell, G. H. Davis, J. P. Bruner, and W. O. Richards, "Robot-Assisted Endoscopic Intrauterine Myelomeningocele Repair: A Feasibility Study," Pediatric Neurosurgery, Vol.36, pp. 85-89, 2002.

[10] T. Kohl et al., "Percutaneous fetoscopic patch coverage of experimental lumbosacral full-thickness skin lesions in sheep," Surgical Endoscopy, Vol.17, pp. 1218-1223, 2003.

[11] R. Nakamura, T. Oura, E. Kobayashi, I. Sakuma, T. Dohi, N. Yahagi, T. Tsuji, M. Shimada, and M. Hashizume, "Multi-DOF Forceps Manipulator System for Laparoscopic Surgery - Mechanism miniaturized & Evaluation of New Interface," Proc. of Fourth International Conference on Medical Image Computing and Computer assisted Interventions (MICCAI2001), Utrecht, the Netherlands, October 14-17, 2001: pp. 606-613, 2001.

[12] K. Nishizawa, and K. Kishi, "Development of Interference-Free Wire-Driven Joint Mechanism for Surgical Manipulator Systems," Journal of Robotics and Mechatronics, Vol.16, No.2, pp. 116-121, 2004.

[13] Y. Haga, and M. Esashi, "Biomedical Microsystems for Minimally Invasive Diagnosis and Treatment," Proceedings of the IEEE, Vol.92, No.1, pp. 98-114, 2004.

Name:
Kanako Harada

Affiliation:
Ph.D student, Department of Mechanical Engineering, School of Science and Engineering, Waseda University; Research resident, Department of Strategic Medicine, National Center for Child Health and Development

Address:
59-307B, 3-4-1 Okubo, Shinjuku-ku, Tokyo 169-8555, Japan

Brief Biographical History:

2001-2003 Production Engineering Research Laboratory, Hitachi Ltd.
2004- Department of Mechanical Engineering, School of Science and Engineering, Waseda University
2005- Department of Strategic Medicine, National Center for Child Health and Development

Main Works:

• K. Harada, K. Tsubouchi, T. Chiba, and M. G. Fujie, "Manipulators for intrauterine fetal surgery in an Open MRI," Proceedings of International Conference on Robotics and Automation 2005, pp. 504-509, 2005.

Membership in Learned Societies:

• Japan Society of Mechanical Engineers (JSME)
• Japan Society of Computer Aided Surgery (JSCAS)

Name:
Kentaro Iwase

Affiliation:
Master Student of Waseda Univ., Graduate School of Global Information and Telecommunication Studies, CIO·IT Course

Address:
5-6-45-401 Toyosu, Koto-ku, Tokyo 135-0061, Japan

Membership in Learned Societies:

• International Academy of CIO (IAC)

Name:
Kota Tsubouchi

Affiliation:
Master Course Student, Visiting Research Associate, Graduate School of Science and Engineering, Waseda University

Address:
3-4-1 Ohkubo, Shinjuku-ku, Tokyo 169-8555, Japan

Brief Biographical History:

2001 Received the B.S Degree from Waseda University
2003- Student in the M.S at Waseda University

Main Works:

• Stabilizer for Fetal Surgery

Membership in Learned Societies:

• Japan Society of Computer Aided Surgery (JSCAS)

Name:
Kousuke Kishi

Affiliation:
Researcher, Mechanical Engineering Research Laboratory, Hitachi, Ltd.; Doctor Course, Department of Mechanical Engineering, School of Science and Engineering, Waseda University

Address:
832-2 Horiguchi, Hitachinaka, Ibaraki 312-0034, Japan

Brief Biographical History:
2001- Mechanical Engineering Research Laboratory, Hitachi, Ltd.
2004- Department of Mechanical Engineering, School of Science and Engineering, Waseda University

Main Works:
• K. Kishi, K. Kan, M. G. Fujie, K. Sudo, S. Takamoto, and T. Dohi, "Dual-Armed Surgical Master-Slave Manipulator System with MR Compatibility," J. of Robotics and Mechatronics, Vol.17, No.3, pp. 285-292, 2005.

Membership in Learned Societies:
• The Robotics Society of Japan (RSJ)
• Japan Society of Computer Aided Surgery (JSCAS)
• Japan Society of Mechanical Engineers (JSME)

Name:
Toshio Chiba

Affiliation:
Director, Department of Strategic Medicine, National Center for Child Health and Development

Address:
2-10-1 Okura, Setagaya-ku, Tokyo 157-8535, Japan

Brief Biographical History:
1986- University of Pittsburgh
1997- The Fetal Treatment Center, University of California, San Francisco
2001- Department of Strategic Medicine, National Center for Child Health and Development

Main Works:
• T. Chiba, "Fetus as Surgical Patient," Journal of Perinatal Medicine, 31:89, 2003.

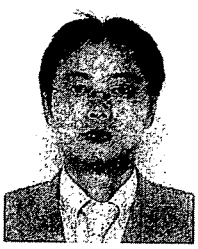

Name:
Tetsuya Nakamura

Affiliation:
Research Engineer, Nanotechnology group, Incubation Center, PENTAX Corporation

Address:
1-9-30 Shirako, Wako-shi, Saitama 351-0101, Japan

Brief Biographical History:
1993 Joined Optical Research Department, Asahi Optical Co., Ltd.
1995- Medical Instrument Division
2001- Incubation Center

Main Works:
• Optics, Medical endoscope

Name:
Masakatsu G. Fujie

Affiliation:
Professor, Department of Mechanical Engineering, School of Science and Engineering, Waseda University

Address:
3-4-1 Ohkubo, Shinjuku-ku, Tokyo 169-8555, Japan

Brief Biographical History:
1999 Doctor of Engineering (in mechanical engineering), Faculty of Engineering, Waseda University
1999- Senior Chief Researcher, Human Care Systems Mechanical Engineering Research Laboratory, Hitachi Ltd.
2001- Professor, Department of Mechanical Engineering, School of Science and Engineering, Waseda University

Main Works:
• Medical robotics
• Welfare mechatronics
• "Development of Exchangeable Microforceps for a Micromanipulator System," Advanced Robotics, Vol.15, No.3, pp. 301-305, Sept., 2001.

Membership in Learned Societies:
• The Institution of Electrical Engineers (IEEE)
• Japan Society of Mechanical Engineers (JSME)
• The Robotics Society of Japan (RSJ)
• Japan Society of Computer Aided Surgery (JSCAS)

産科と婦人科　別刷

Vol. 73 No. 4（2006年4月1日発行）

発行所　株式会社 診断と治療社

胎児閉塞性尿路疾患の周産期管理と治療（3）

国立成育医療センター特殊診療部 千葉敏雄（ちばとしお）
同 第二専門診療部泌尿器科 上岡克彦（かみおかかつひこ）

はじめに

膀胱拡張（megacystis, enlarged bladder）は，一般には閉塞性尿路疾患 obstructive uropathy の代表的症候とされるが，実際にはその成因は，1）器質的閉塞 bladder outlet obstruction によるもの，2）非閉塞性機序 nonobstructive causes によるものとに分かれる．前者は羊水過少を呈しやすく，一部は子宮内 intervention の適応となる点を特徴とするが，後者では羊水量は通常正常域内にあり，かつ，（尿路自身に対する）子宮内 intervention の適応からは除外される．後者に属する神経因性膀胱（脊髄髄膜瘤など）等にも一部触れるが，本稿では主に，胎児閉塞性尿路疾患に対する子宮内 intervention につき述べることとしたい．前稿に述べたように，骨盤内胎児腫瘍（仙尾部奇形腫など）もまれながら，（骨盤内腫瘍の圧迫による）尿路閉塞をきたして胎児手術の適応となる[1]．このような外因性の胎児尿路閉塞に対するものを例外的と考えれば，一般の子宮内 intervention はいずれも，尿路減圧による患児の出生後予後改善を目的とするものである．それらは手技的には，1）閉塞した尿流をバイパスさせるもの（シャント留置術，特に膀胱羊水腔シャント術 vesicoamniotic shunting），2）尿流閉塞部位自体での原因を解除するもの（尿路閉塞解除術）とに分けられるが，両者間にはその期待される効果において明らかな相違がある．前者の vesicoamniotic shunt は，腎を中心とする上部尿路機能の改善・維持に主眼を置くのに対し，後者，たとえば後部尿道弁（PUV）に対する直接的閉塞解除は，腎のみならず一定の膀胱機能を生後長期間期待する（後述）ためのものである．以下，本稿では，これらのポイントについて，その現状と今後を述べてみたい．

閉塞性尿路疾患に対する子宮内 intervention の手技

閉塞性尿路疾患に対する子宮内 intervention は，Harrison らが施行した胎児直視下の両側尿管瘻造設術が最初のものである[2]．この症例は，両側水腎症と羊水過少を呈する 21 週の胎児 PUV 症例で，結果的には患児は両側腎不全と肺低形成により死亡している．その後も尿路閉塞に対する胎児手術（膀胱瘻など）が行われているが，子宮切開による直視下尿路減圧手術は，現在までのところ Harrison グループによる数症例にほぼ限られている．一方，胎児尿路系への子宮内 intervention は全体としてその数を増しており[3]，その臨床的意義についても種々の議論がなされてきた．この子宮内 intervention

0386-9792/06/¥100/頁/JCLS

は近年，超音波ガイド下（vesicoamniotic shunting）あるいは胎児内視鏡下のものとなっている（含，レーザー治療など）．その際，母体全麻は必須とはいえず，施設によっては母体への局麻剤（母体腹壁）と鎮静剤（経静脈性；経胎盤的な胎児鎮静も得られる）投与にて，子宮内 intervention が完遂されることも多い（母体硬膜外麻酔や直接的胎児鎮静・筋弛緩投与も通常は行われていない）が，感染予防のために抗菌薬は常に使用される．子宮内 intervention が診断あるいは治療的なもののいずれであっても，また治療的 intervention が超音波ガイド下あるいは内視鏡下のいずれにしても，胎児閉塞性尿路疾患で高率に随伴する羊水過少の存在は，手技上の大きな問題となる．

同時に，子宮内 intervention を行うタイミングも大きな問題といえる．近年，妊娠早期の megacystis に対し 10～14 週で膀胱穿刺 vesicocentesis を行ったとする報告[4]や，1st trimester に PUV に対する vesicoamniotic shunting を施行したとする報告[5]もあり注目される．妊娠早期の megacystis は自然縮小する可能性もあり，この時期の intervention は控えるべきとする考えがある[6]一方，megacystis の臨床経過は妊娠前半と後半発症とでは異なるものであり，前半発症の場合には子宮内 intervention の有無にかかわらず予後不良とする報告もみられる[7]．この報告では，megacystis の子宮内自然軽快例のなかにも出生後腎不全（腎移植）となった症例が含まれており，極めて興味深い．ただ，全般的な近年の考え方は，閉塞性尿路疾患で子宮内 intervention を施行すべき症例は限られたものであり，最近の試算で胎児 60,000 例に約 1 例という見解も出されている．したがって，胎児閉塞性尿路疾患に対する子宮内 intervention は，今後も一定の限られたセンターで施行され評価を受けることが望ましいといえる．

1. Vesicoamniotic shunting[6][8]

1）手技の実際

この intervention はすでに述べた通り，胎児尿流の羊水腔への simple diversion による preventative な手技であり，決して curative なものではない．実際に施行するに際しては，事前に十分胎盤，胎児の位置を確認し，可能な限り胎盤穿刺ルートは避けるべきである（やむを得ない場合，経胎盤的穿刺も行われるが，その際は color Doppler 併用にて chorionic plate 上の胎盤表面血管を避ける）．しばしば合併する羊水過少 oligohydramnis/anhydramnios は，超音波による子宮腔内描出や胎児内視鏡操作のうえで，あるいは留置される shunt stent 遠位端の位置確認のうえで，技術的に大きな不利をもたらす．したがって，手技的には，超音波ガイド下に子宮腔を穿刺し（fluid leakage 低減上，主に子宮底部より行う），一定量の加温 L-R 液を注入することで羊水腔/ポケットを reexpand しておく（amnioinfusion；通常 300～500 m*l*）ことはしばしば有用である．また，常に color Doppler を併用して子宮腔内の臍帯（通常，狭小な羊水ポケット内に存在）とその血管に対する誤穿刺を避ける．この穿刺にあたっては，子宮底部からの直線的アプローチ（手技的に容易で術後羊水 leakage が少ない）が可能となるように，胎児はできるだけ背臥位（back-down）で頭頂位（vertex presentation）にあることが望ましい．もしこのような胎位にない場合は，external manipulation の施行に限ることなく，種々の方法（母体歩行，母体体位変換，手技施行の延期等）を試みることも重要である．また，望ましくない胎位で子宮下部穿刺を行う場合は，羊水 leakage をきたすリスクも高くなることから，術後 72 時間は母体を十分な安静臥床におく必要がある．

胎児の膀胱穿刺 vesicocentesis に際しては，常に胎児下腹壁を目指し（恥骨枝直上で正中を

はずした側方より），かつ color Doppler にて拡張膀胱両側を横走する臍動脈分枝を避けつつ，膀胱下部を穿刺する．この膀胱下部を穿刺すべき理由は，1）膀胱サイズが vesicocentesis の操作中に縮小 shrink してくる（すなわち，貯留尿 drainage とともに膀胱全体は下方・骨盤腔に落ち込んでゆく）ため，膀胱上部穿刺では尿 drainage が不十分に終わる可能性があること，また 2）本 shunt において高頻度にみられる shunt catheter displacement を防止するためでもある．この 2）の意味を理解するためにはまず，胎児膀胱は一般に尿貯留とともに骨盤側より頭側に（“dome 状に”）拡張してゆくことを知らねばならない（**図 1-A**）．その場合，もし shunt catheter が拡張膀胱高位に刺入されていれば，shunt catheter 留置により膀胱の drainage/減圧・サイズ縮小が進行するとともに膀胱上部壁（catheter 刺入部）が胎児骨盤腔

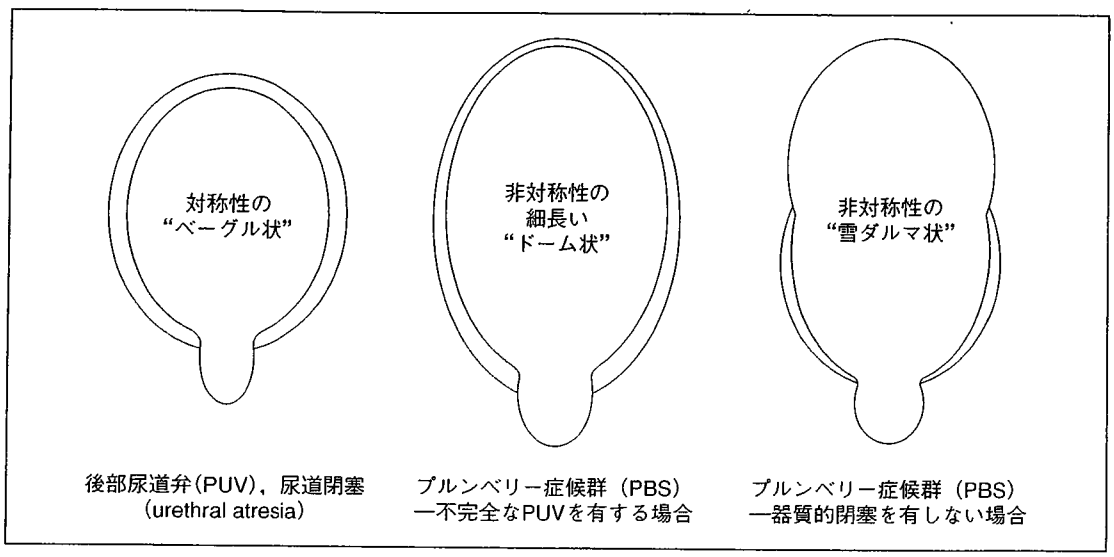

図 1-A　胎児閉塞性尿路疾患における拡張膀胱の超音波画像所見　(from Johnson MP)

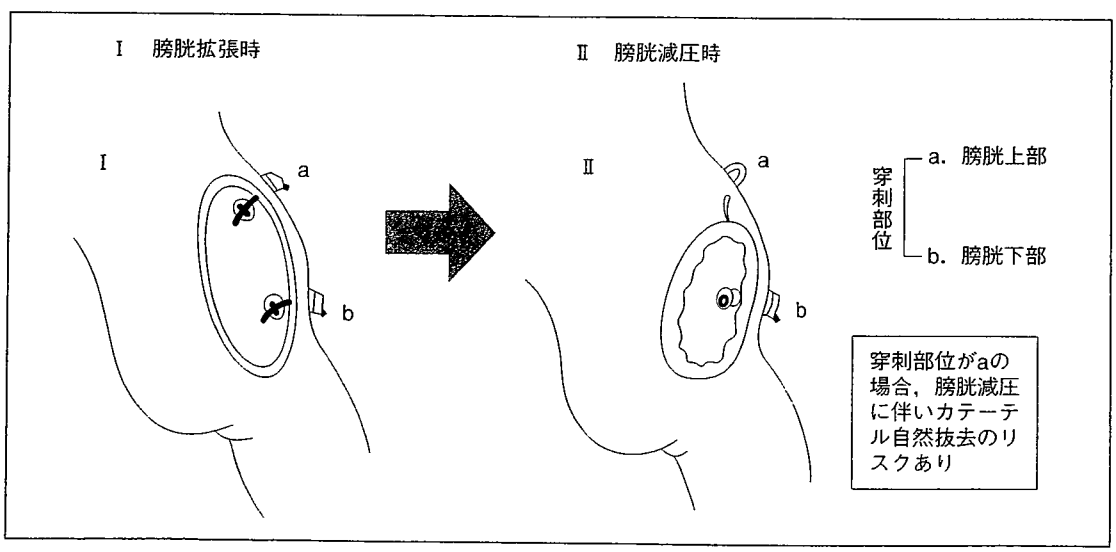

図 1-B　閉塞性尿路疾患に対する vesicoamniotic shunt 留置時の胎児腹壁穿刺部位の重要性

(from Johnson MP)

に落ち込んでゆき，大きな張力/牽引力がshunt catheterに加わることでcatheter近位端(proximal end，本来膀胱腔内に位置する)が膀胱より胎児腹腔内にdisplace・抜去され，(patentな膀胱穿刺孔よりの)尿leakage/urinary ascitesをみることになる(megacystis再発)(図1-B)．

実際の臨床上，shunt操作に用いる器具(shunt apparatus)には，いわゆる“コイル型(double pigtail catheter)”のもの，特にHarrison fetal bladder stent (Cook, USA)あるいはRodeck vesicoamniotic shunt catheter (Rocket, UK)，あるいは“ダブルバスケット型”のもの(内瘻化カテーテル，Hakko)が用いられてきている．各々特徴を有し(詳細は他の文献参照)，施設により使用されるカテーテルも異なっている．いずれのapparatusを用いるにせよ，十分な習熟はshunt displacementなどの手技的合併症を防止するうえで不可欠である．Shunt catheter留置後は，そのcoiled(あるいはバスケット状)segment(proximal/distal)の位置，および膀胱drainageの状況は，超音波検査にて確認可能である．本shunting術後は適宜，子宮収縮モニタリング(external fetal/uterine monitoring)を行い，uterine irritabilityが明らかであれば，必要に応じてtocolytic therapyを付加する(routineには使用されてはいない)．術後follow-up(施設，術者によっては入院せず外来のみ)では，1，2日でcatheterの位置，機能を観察し，その後少なくとも6～8週間は毎週これをチェックすることで尿路系の拡張と羊水量を記録してゆき，問題がなければその後2週に1度とする．この間，妊娠28週前後に達すれば，常に小児泌尿器科医や新生児科医とのconsultationを行い，出生後の管理方針につき検討を開始しておくことが必要となる．閉塞性尿路疾患患児の妊娠経過では，子宮内shunting施行の有無にかかわらずやや早期産となる傾向がみられる(自然破水等)が，分娩は帝切の産科的適応がなければ経腟自然分娩で行われる．

2) 合併症

胎児のvesicocentesisによるpregnancy loss率(0.5～1.0%)は，通常のamniocentesisと基本的に変わるものではない．しかしvesicoamniotic shuntingではより高いと考えられ，以下の産科的合併症のリスクは常に考慮されねばならない．すなわち，chorioamnionitis等，羊膜剝離・破水(PROM)，intraplacental bleeding(transplacental approachをとった場合)，術後子宮収縮(preterm labor)・早産などである．次に，産科的合併症とは分けて手技的合併症についても考えねばならない．その中には，胎児・胎盤の位置等によるshunt catheter留置困難とcatheterの位置異常，留置catheterによる合併症(閉塞・事故抜去，および膀胱尿leakageとurinary ascitesなど)，catheter留置に伴う合併症，胎児への直接的外傷やcatheter留置持続に伴う周囲組織(胎児前腹壁等)の損傷などが報告されている．それらのなかで代表的なものは，やはりshunt catheter diaplacementであり(30～45%)，その場合しばしばcatheter再留置を要する．このshunt catheter displacementの主因は近年，その羊水腔内segment(distal/intra-amniotic)が胎児四肢に絡まることによる自己/事故抜去(ないしdislodgement)と考えられるようになった．もう一つの原因は，shunt catheterが拡張膀胱(dome状)高位に刺入されていた場合，膀胱の減圧・サイズ縮小とともに起こりうるcatheter proximal endの腹腔内dislodgementである(図1-B)．このcatheter displacement以外の手技的合併症には，vesicocentesisに伴うvesicoperitoneal fistula(およびurinary ascites)があり，その多くは一過性で1，2週間で自然閉鎖(およびmegacystis

が再発）する可能性も高い．さらに，多量のurinary ascites貯留が遷延する場合，持続的な胎児腹壁distentionが，腹壁に非可逆性の組織学的変化（いわゆるprune belly phenotype）をきたすこともある．最後に，たとえshunt留置が手技的に成功しても，5%でIUFDが生じたという報告[9]にも関心がよせられている．

2. 尿路に対する直接的閉塞解除術

前述の単なる膀胱減圧術（shunt catheter留置）のみならず，尿道における直接的閉塞解除も行われるようになっている．これは胎児内視鏡による（あるいは超音波ガイド下の）直接的な尿路通過障害解除術である．このような手技も選択肢として考慮・施行されるようになった理由として，主に以下の2点が挙げられる．1つには,shunt catheter留置術における諸問題（上述）に伴い，その効果がまれならず不確実なことである．2番目に指摘されることは，shunt留置による拡張膀胱の減圧のみでは，たとえ上部尿路（腎・尿管）機能障害は予防ないし改善し得ても，膀胱機能障害が出生後長期間遷延する可能性を残すことである．その理由は，胎児膀胱の発達には，生理的な“蓄尿—排尿サイクル”の存在が必須であり[9]，膀胱へのshunt留置・減圧のみでは膀胱発達にとって重要なこの因子が失われるためである．

経皮的超音波ガイド下の直接的閉塞解除術としては，胎児内視鏡（胎児膀胱鏡）による手技がQuinteroら[10)~12)]により，胎児PUV症例でのレーザーないし電気的な尿道弁焼灼・切開術として報告されている．その後同様の胎児膀胱鏡手技が，温生食水圧注ないし軟性guide wireによる鈍的穿通手技[13]として，試みられている．このような手技は，多くは超音波ガイド下に胎児膀胱内に留置された細径内視鏡にて，内尿道口・尿道弁を順方向に観察しつつ行われている（fetal antegrade cystourethroscopy）．ここでわれわれが理解すべきことの一つは，膀胱内腔から観察される近位尿道は，子宮内での胎児成長・発達に伴い観察視野が変化してくるということである．そしてその理由は，近位尿道起始部長軸の膀胱に対する角度・方向（antegrade angle）が，妊娠週数に伴い変化してゆくことにある．すなわち，妊娠早期（14～16週）では近位尿道が膀胱に対して角度のつくことなく（いわばstraightに）起始するものの，妊娠20～24週に至れば，このantegrade angleがかなり明確になってくるのである（図2）．したがって（産科的合併症のリスクを別とすれば）いったん膀胱腔に適切な方向で入れば，妊娠早期では近位尿道内腔を内視鏡にて観察することは容易であるのに対し，妊娠の進行にともない同様のアプローチはその困難さを増してくる．このことは，かかる胎児内視鏡手技によるPUVの（antegrade）尿道弁切開術完遂に一定の影響を及ぼすものと考えられる．

一方，このような内視鏡的antegrade手技に対し，Soothillらは，内尿道口に陥入し尿流閉塞をきたした尿管瘤ureteroceleに対し，超音波ガイド下のみにて（内視鏡を使用せずに）レーザー焼灼・穿孔（接触方式）を試み，臨床的な成功をおさめている[14]．

われわれも，貯留尿により巨大嚢胞化した尿道憩室のために完全尿路閉塞（megacystis，羊水過少）を呈した妊娠19週の胎児前部尿道弁症例に対し，胎児内視鏡（羊水腔内）による嚢胞状憩室壁のレーザー穿孔術（接触式ablation）を行い，閉塞の解除（羊水過少の寛解）をみている（ただし，児は術後chorioamnionitis併発によるIUFDをきたした）．われわれは，このような病態に対するより低侵襲性の手技（たとえばhigh-intensity focused ultrasound, HIFUなど）導入により，将来はいっそうの治療成績改善が望めるものと期待している．